acta phys. slov. 30. (1980), No. 4

INDUCED ANISOTROPY AND OTHER MAGNETIC PROPERTIES OF Mn—Cr SPINELS*

SVATOPLUK KRUPIČKA**, ZDENĚK JIRÁK**, PAVEL NOVÁK**, FRANTIŠKA ZOUNOVÁ**, VLADIMÍR ROSKOVEC***, Praha

Measurements of the induced anisotropy, magnetocrystalline anisotropy, rotational hysteresis, magnetic moment and Curie temperature in the spinel system $Mn_{1+x}Cr_{2-x}O_4$ $(0 \leq x \leq 2)$ are reported. Three distinct sources of the induced anisotropy were found. Two of them are connected with the presence of the Jahn-Teller Mn^{3+} ions, the third one is a consequence of the long range spiral spin arrangement of the Cr^{3+} ions.

НАВЕДЕННАЯ АНИЗОТРОПИЯ И ДРУГИЕ МАГНИТНЫЕ СВОЙСТВА Mn—Cr ШПИНЕЛЕЙ

В работе описаны измерения наведенной анизотропии, магнитокристаллической анизотропии, вращательного гистерезиса, магнитного момента и температуры Кюри шпинелей $Mn_{1+u}Cr_{2-x}O_4$ $(0 \leq x \leq 2)$. Были обнаружены три разные источника неведенной анизотропии. Два из них связаны с наличием в системе Ян-Теллеровских ионов Mn^{3+}, третий является следствием дальнодействующего спирального упорядочения спинов ионов Cr^{3+}.

I. INTRODUCTION

From the crystallochemical point of view there are some similarities between the system of spinels $Mn_{1+x}Cr_{2-x}O_4$ $(0 \leq x \leq 2)$, and the more frequently studied system $Mn_{1+x}Fe_{1+x}O_4$. In both cases the structure is cubic for manganese-poor, and tetragonally distrorted for manganese-rich compositions and in both a miscibility gap exists in the equilibrium phase diagram, where the tetragonal and cubic phase coexist [1—6]. The tetragonal distortion is due to the cooperative Jahn–Teller effect of Mn^{3+} ions in the octahedral (or B) sublattice [7]. By rapid cooling from high temperatures a continuous series of one phase solid solutions throughout the whole compositional range $0 \leq x \leq 2$ may be prepared in both systems [2, 4, 5]. At low temperatures these are tetragonal with x exceeding a certain critical value x_c

* Dedicated to Academician Vladimír Hajko on the occasion of his 60th birthday.

** Institute of Physics, Czechoslovak Acad. Sci., Na Slovance 2, CS-180 40 PRAHA.
*** Present address: Výzkumný ústav matematických strojů, Lužná 2, CS-160 00 PRAHA.

and cubic for $x < x_c$. In Mn-Cr spinels x_c was found to be approximately 0.8 at room temperature [5] and 0.7 at 4.2 K [8]. Due to a strong preference of both Cr^{3+} and Mn^{3+} for the octahedral coordination [9, 10], the Mn—Cr spinels are normal, i.e. the corresponding formula is $Mn^{2+}[Mn_x^{3+}Cr_{2-x}^{3+}]O_4$, as confirmed by the neutron diffraction [11].

Unlike the crystallographic properties the magnetic ones and especially the magnetic structure of $Mn_{1+x}Cr_{2-x}O_4$ differ considerably form those of Mn—Fe spinels. Particularly in the chromite system the $A-B$ superexchange interactions are relatively weak. This leads to a rather low Curie temperature (about 40 K) and, due to the competing $B-B$ interactions, a noncollinear spin structure appears.

The magnetic structure of $MnCr_2O_4$ was studied by several authors using both the neutron diffraction [12—15] and the NMR [16] methods. The results were usually discussed with respect to the predictions of the Lyons–Kaplan–Dwight–Menyuk theory [17] of the spiral ground state spin configuration in spinels. The most recent neutron diffraction study of Vratislav et al. [15] has confirmed the ferrimagnetic three-cone spiral to be at least a good approximation to the ground state of the stoichiometric manganese chromite, admitting that the propagation vector of the spirals deflects somewhat from the ⟨110⟩ direction. This structure changes at $T_k = 16$—18 K to a collinear one in the sense that the long range order of the transversal components of spins disappears and only the short range order persists. Due to this character of the phase transition only a very small change of the overall magnetization may be observed at T_k [15]. A similar situation arises if the chromium ions are gradually replaced by Mn^{3+}; a small concentration of manganic ions ($x \leq 0.05$) is then sufficient to destroy the long range spiral configuration so that only a short range order of noncollinear spins remains in the whole temperature range $0 \leq T \leq T_c$.

When approaching the other end member, i.e., Mn_3O_4, a Yafet–Kittel-like spin structure appears [18—21]. This is characterized by a doubling of the magnetic unit cell in the ⟨010⟩ direction of the tetragonal b. c. lattice leading to an overall orthorhombic symmetry. According to Jensen and Nielsen [20], there is a magnetic transition in Mn_3O_4 at 33 K, above which those Mn^{3+} spins that give rise to the magnetic cell doubling at lower temperatures form a spiral. The long-range Yafet–Kittel arrangement was observed also in $Mn_{2.5}Cr_{0.5}O_4$ [21]. It seems, therefore, that this structure is less sensitive to the presence of the substitutional spins compared with the spiral.

In spite of the fact that the type of the low temperature spin arrangement has been determined with a satisfactory accuracy at least for both end members $x = 0$ and $x = 2$, some controversy still remains concerning the exact values of the cone angles as well as the magnitude of the magnetic moments of ions [12, 13, 15, 16].

Another point of interest with the Mn—Cr system are strong relaxation effects. These manifest themselves, e.g., by a rotational hysteresis discovered first in

nominally stoichiometric $MnCr_2O_4$ by Miyahara et al. [22]. They were tentatively ascribed to friction connected with the movement of boundaries separating domains characterized by different propagation vectors of the spiral structure, when the direction of the overall magnetization is being changed. In paper [23] we have shown, however, that the appearance of the rotational hysteresis at low temperatures is conditioned by the presence of Mn^{3+} ions ($x > 0$), being at least for small x values proportional to x and vanishing for $x \to 0$. An interpretation has been proposed based on the assumption that a strong coupling exists between the spin system and the local Jahn–Teller distortions of Mn^{3+}-occupied octahedra. A further investigation [24] has supported this basic idea. At the same time, however, it has revealed a large complexity of the relaxation effects in Mn—Cr spinels requiring a refinement and extension of the interpretation.

The main aim of the present paper is to give a full account of our study of the relaxation effects in the system $Mn_{1+x}Cr_{2-x}O_4$, $0 \leq x \leq 2$. As they prove to be intimately connected with the magnetic anisotropy and its relaxation, including the effects of annealing and/or cooling in the magnetic field, it is reasonable to treat all these phenomena together on a common basis and actually as the one topic only. Preliminary results were published in [25].

In addition, to obtain a more complete picture of the magnetic properties of the studied system, we have also performed the measurements of magnetization including its dependence on the temperature, the magnetic field and the composition.

II. EXPERIMENTAL

II.1. Samples

Single crystals of cubic symmetry, having compositions within the limits $0.04 \leq x \leq 0.55$, were grown by the flux method using Bi_2O_3—V_2O_5, Bi_2O_3—B_2O_3 and PbO—PbF_2 melts [26]. The attempts to prepare single crystals with $x > 0.04$ were unsuccessful. The tetragonal single crystals of Mn_3O_4 were also grown from the Bi_2O_3—V_2O_5 flux. The polycrystalline samples were prepared by usual ceramic technique from homogenized $MnCO_3$ and Cr_2O_3 mixtures. After calcination at 700 °C the materials were carefully homogenized again, pressed into pellets and sintered either in air for 24 hours at 1350 °C ($x \geq 0.2$), or in a vacuum of 10^{-3} Pa at 1450 °C for 10 hours ($x > 0.2$). The latter procedure was used in order to avoid oxidation and decomposition of the samples. The samples were then rapidly cooled down in air. The room temperature X-ray diffraction patterns corresponded in all cases to a single spinel phase, cubic for $x < 0.8$ and tetragonal for $x \geq 0.8$. The chemical composition was checked by chemical analysis and by measuring the lattice parameters. The accuracy of determination of x was usually ± 0.01 and in the case of small single crystals ± 0.02. The oxygen stoichiometry was checked selected test compositions and found to be within ± 0.02 per f. u. (i.e., 0.5 % of the total oxygen content) [27]. For magnetic measurements spheres of diameter 2—5 mm were ground.

II.2. Magnetization measurements

Magnetic moments were measured by the ballistic method in the temperature range 2—80 K, for magnetic fields up to 4.2 T. In some cases, complementary measurements were made using the pulse fields up to 15 T. The pulse duration was 9 msec. Some additional experiments were also performed on the vibrational magnetometer in the Institute of Physical Problems in Moscow.

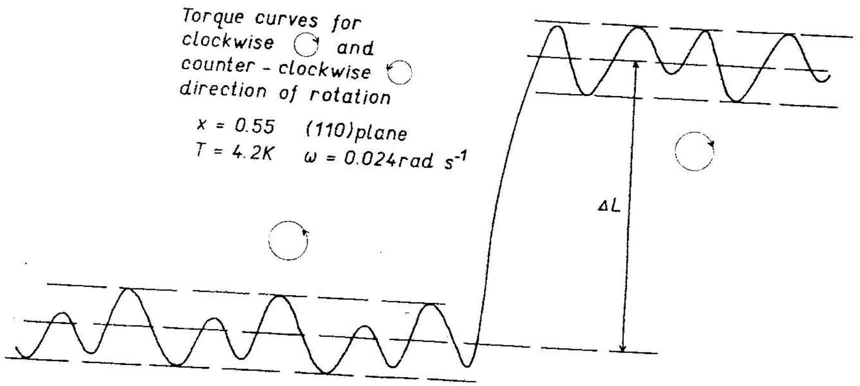

Fig. 1. Definition of the rotational hysteresis ΔL.

II.3. Torque measurements

The measurements were carried out using an automatic compensated torquemeter [28] with a rotable electromagnet yielding fields up to 1.6 T. The speed of the rotation could be varied within the limits $0.024 \text{ rad s}^{-1} \leqslant \omega \leqslant 0.276 \text{ rad s}^{-1}$, or the magnet was operated manually in the case when a fast (quasiadiabatic) change of the field direction was needed. Usually the field 1.2 T was used, which is sufficient to saturate at least the cubic samples.

The measured quantities were:

(1) The angular dependence of the torque from which the anisotropy and, eventually, also its time change could be determined. For these measurements the sample was usually cooled in a magnetic field, in order to reach a single domain behaviour.

(2) Rotational hysteresis defined as the difference between the average torque values traced for a clockwise and counterclockwise rotation of the magnet (see Fig. 1)

$$\Delta L \equiv \langle T_{\circlearrowright} \rangle - \langle T_{\circlearrowleft} \rangle . \tag{1}$$

For this type of measurements the samples were cooled without an external magnetic field or else a rotating field was applied. (When cooling in a constant field ΔL was systematically higher by 5—10 %).

(3) The time change of the torque for a given direction of the magnetic field; here an anisotropy was induced by cooling the sample in a magnetic field and then the field was quickly turned to the new direction.

III. RESULTS

III.1. Magnetic moments and Curie temperatures

Measurement of magnetization were carried out on samples with 12 different compositions, three of these samples were single crystals. In the latter case the magnetic field was applied along the $\langle 111 \rangle$ direction. The spontaneous magnetization was determined by either extrapolating for $B_0 = \mu_0 H \to 0$ (at low temperatures) or by using the method of thermodynamical coefficients [29] for higher temperatures close to T_c, where the paraprocess is important (Fig. 2). In the latter case $M(H=0)$ was determined by plotting H/M vs. M^2 and extrapolating the linear dependence obtained to $H/M = 0$ (Fig. 3). In the tetragonal samples ($x \gtrsim 0.7$) a strong uniaxial anisotropy makes the technical saturation difficult, thus it was necessary to use the pulse fields. From the temperature dependence of the spontaneous magnetization the Curie temperature was obtained, as plotted in Fig. 4. In the same figure the magnetic moments at 4.2 K are displayed for several values of the external magnetic field.

Besides the normal paraprocess a strong field dependence of magnetization is clearly visible even at low temperatures. This may be attributed to the noncollinear spin structure; related volume susceptibility of the paraprocess $\chi = \Delta M/\Delta H$, was found to be 2—4×10^{-3} (SI units).

III.2. Rotational hysteresis

The appearance of the rotational hysteresis may be connected either with the relacation processes [30, 31] or with the magnetization processes in the nonsaturated region [32]. In the first case, the effect exists also when saturation is complete, while the second kind of rotational hysteresis should disappear in fields exceeding approximately the twofold value of the effective anisotropy fields.

In order to verify the relaxation origin of the effect studied, the rotational hysteresis was first measured as a function of the applied magnetic field. In the cubic region the saturation of ΔL was achieved in relatively low fields $\lesssim 0.5$ T and ΔL remained constant up to the maximum field in our measurements. In the tetragonal region the anisotropy is considerably larger and the saturation of ΔL was not complete in all cases. In spite of this the character of the ΔL vs. B_0 curves indicates that the contribution of nonrelaxing processes to ΔL — if any — remains small (Fig. 5).

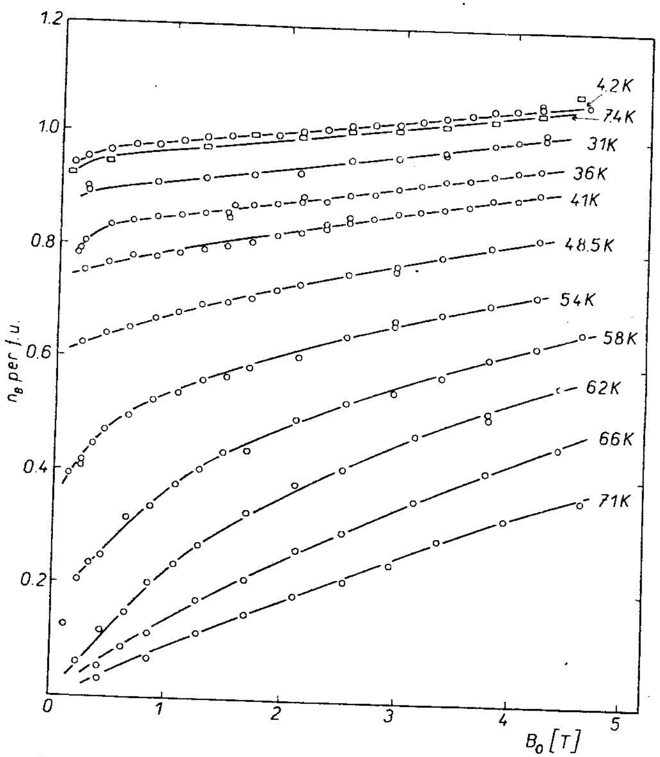

Fig. 2. Dependence of the magnetization on the magnetic field for the single crystal $Mn_{1.55}Cr_{1.45}O_4$.

The relaxation origin of the rotational hysteresis manifests itself also in temperature and frequency dependences of ΔL (Fig. 6). In accordance with the theoretical predictions, the ΔL vs. T curves exhibit a maximum which could be clearly detected at least in some cases, i.e., for compositions close to the end members of the series. For the x's inbetween, the position of the maximum is shifted towards lower temperatures, not accessible to our experiment. This corresponds to shorter

Fig. 3. Dependence of H/M on M^2 for $Mn_{1.55}Cr_{1.45}O_4$.

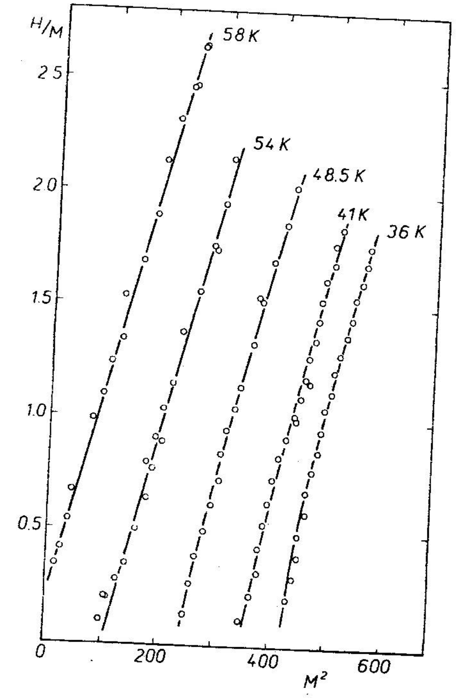

relaxation times, as observed also in our torque measurements (§ III.3). The height of the maximum ΔL_{max} was taken as the measure of the magnitude of the relaxation. The dependence of ΔL_{max} on x is shown in Fig. 7.

III.3. Torque measurements

It follows from the theoretical considerations that the rotational hysteresis described in the previous section shall be accompanied by an induced anisotropy possessing short relaxation times even at low temperatures. The first aim of the torque measurements we shall describe now was to study this anisotropy in some detail. Besides, other anisotropy effects were observed and analyzed in order to get a complete picture.

a) Polycrystals

In agreement with the absence of the rotational hysteresis in stoichiometric $MnCr_2O_4$ no induced anisotropy, fast relaxing at low temperatures, was detected in this case. On the other hand, an induced anisotropy (labelled by II in Fig. 7) stable up to approx. 15 K could be induced by cooling the sample in the magnetic field. The anisotropy is uniaxial $F_A = K_u \cos^2\vartheta$ with K_u (4.2 K)≈ 2 kJ/m^3 (2×10^4 erg-/cm^3)[1]), slightly depending on the cooling rate in the critical region between approx. 20 and 15 K. With rising temperature K_u gradually decreases being at 16 K about 2/3 of its 4.2 K value. At this temperature the direction of the easy axis can be changed by changing the direction of the external magnetic field. No anisotropy was detected above 18 K.

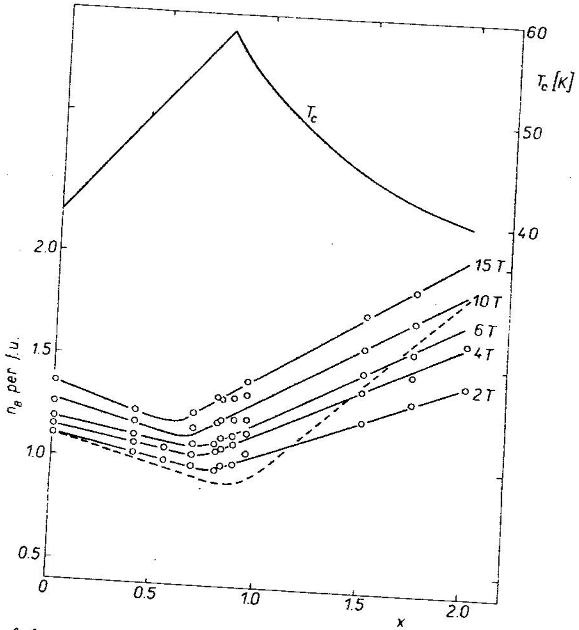

Fig. 4. Dependence of the magnetic moment and of the Curie point T_c in the $Mn_{1+x}Cr_{2-x}O_4$ system. The spontaneous moment derived from the present and other data is marked by the dashed line.

The anisotropy of the type described above was observed also for compositions with $x \neq 0$ but close to the stoichiometric one; it practically vanishes for $x \gtrsim 0.07$. At the same time, another uniaxial contribution to the induced anisotropy emerges, as seen in Fig. 7 (labelled by III). It increases with x, exhibits a maximum $K_u \approx 1.6$ kJ/m^3 at $x \cong 0.7$ and drops in the tetragonal region.

For $x \neq 0$ an induced anisotropy fast relaxing at low temperatures, identified to be of the same origin as the rotational hysteresis, was observed throughout the

---

[1]) When evaluating the torque measurements described in [25] a wrong multiplicative factor was used. This mistake is corrected in the present paper.

Fig. 5. Dependence of the rotational hysteresis ΔL in $Mn_{1+x}Cr_{2-x}O_4$ on the magnetic field.

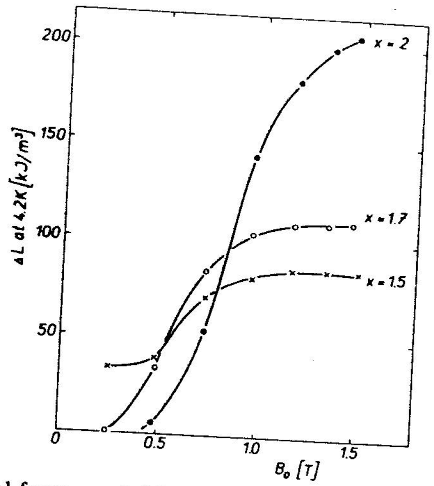

whole compositional range $x \leq 2$. An unusual feature of this anisotropy is that, in addition to a uniaxial part, it possesses a unidirectional component of a comparable magnitude. This is clearly seen from a typical torque curve shown in Fig. 8.

The relaxation behaviour of both these components is practically the same as demonstrated in Fig. 9. Here, the time dependence of the first and the second Fourier coefficients a_1, a_2 of the torque curve is shown for the given temperature ($T = 1.75$ K) besides their temperature dependence (measured during the first turn over of the magnet). This anisotropy (we denote it as I) can be induced only at low temperatures, as indicated in Fig. 9. The mean relaxation times τ were estimated from the time dependences of the torque curve; e.g., for $x = 0.2$ we found τ to be ≈ 120 sec and 5 sec at 1.75 and 4.2 K, respectively. This may be compared with $\tau \approx 30$ sec at 2.5 K, deduced from the position of the ΔL_{max} for this composition. This agreement of the relaxation behaviour points to the same origin of anisotropy I and the rotational hysteresis, but the values of τ cannot be taken too literally because the relaxation process is too complex to be described by a single relaxation time (see Appendix I). This manifests itself also in the experiments with a quasiadiabatic change of the field direction. The relaxation of the induced anisotropy was then much slower compared with the case of continuous rotation and, moreover, its rate was found to depend on the angle of rotation.

The critical temperature regions, in which anisotropies I, II, III may be induced (or changed) in a reasonable time (up to ≈ 1 hour), are indicated in Fig. 10.

B) Single crystals

With regard to the strong relaxation effects the cubic anisotropy was determined from the temperature dependence of the torque consecutively measured in various fixed directions. As compared with the previously published data [23], the measurements were completed and the results reevaluated. These are shown in Fig. 11. Most measurements were performed in the (110) plane. The anisotropy constant K_1 was evaluated from Fourier coefficients at $\sin 4\varphi$ and $\sin 6\varphi$; the coefficient at $\sin 2\varphi$ was omitted because of the presence of rather strong induced uniaxial anisotropy terms. A comparative measurement in the (001) plane for the

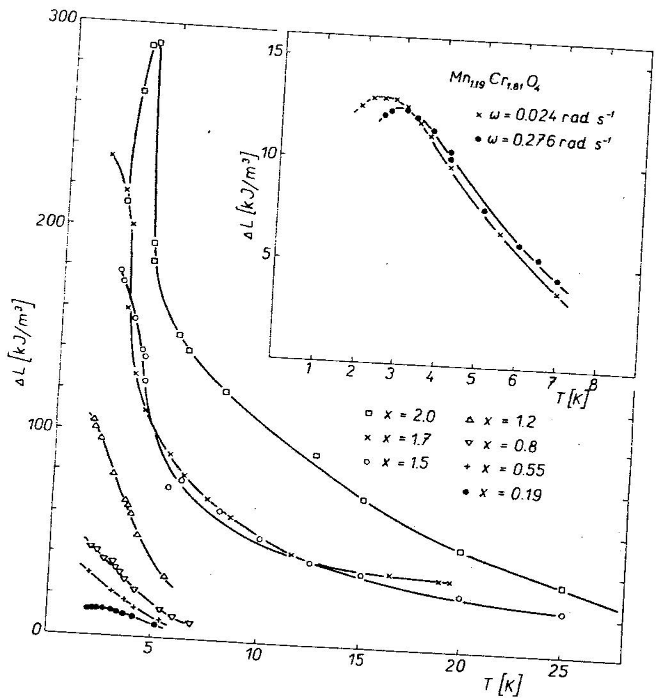

Fig. 6. Temperature dependence of the rotational hysteresis ΔL in $Mn_{1+x}Cr_{2-x}O_4$. The influence of the frequency is shown in the insert.

sample $x = 0.55$ confirmed the reliability of this procedure. Above approximately 10 K the constant K_1 obtained in a more conventional way by directly measuring the torque curve during the rotation of the magnet shows the same qualitative behaviour. The quantitative differences may be connected with the fact that, in the presence of a relaxing anisotropy, the quantities measured in the two procedures described need not be identical.

As to the relaxing part of the anisotropy, the effects found in single crystals are fully analogous to those in polycrystals. Therefore, we shall limit ourselves to some

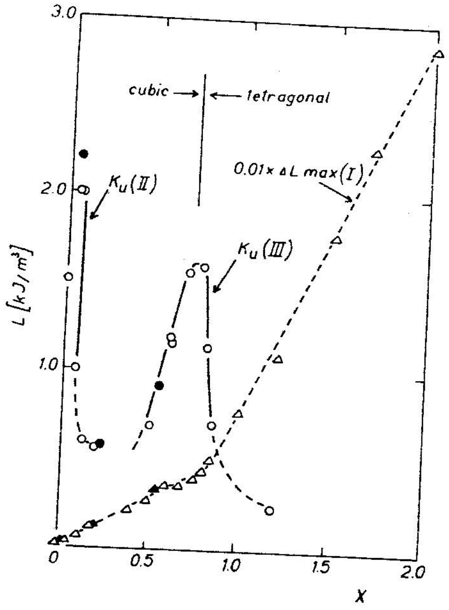

Fig. 7. Induced anisotropy of the processes I, II, and III characterized by the maximum rotational hystresis ΔL_{max} (I) and by the constant K_u (II, III) at 4.2 K ($L = -K_u \sin 2\varphi$) in the system $Mn_{1+x}Cr_{2-x}O_4$. Full points: single crystals, open points: polycrystals.

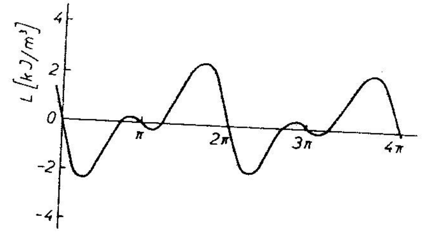

Fig. 8. Torque curve for the polycrystal $Mn_{1.2}Cr_{1.8}O_4$ at 1.75 K. The contribution of a unidirectional term is clearly visible.

additional information concerning mainly the symmetry of the induced anisotropies I, II, III, which cannot be deduced from measurements on polycrystals.

Anisotropy I can be induced in any crystallographic direction. Its magnitude seem to increase slightly when proceeding from the ⟨100⟩ to the ⟨110⟩ direction; the results were, however, very sensitive to the detailed course of the cooling procedure. Anisotropy II could be studied on a single crystal with $x = 0.04$ only. Even in this case it was partly obscured by the effect I of comparable magnitude. After subtracting the latter and the cubic anisotropy as well, the qualitative conclusion can be drawn that the magnitude of II is largest for the ⟨110⟩ direction. Anisotropy III was measured on a single crystal with $x = 0.55$. It was expressed in the usual form

$$F_A = -F \sum_{i=1}^{3} \alpha_i^2 \beta_i^2 - G \sum_{i>j=1}^{3} \alpha_i \alpha_j \beta_i \beta_j , \qquad (2)$$

where α_i's and β_i's are the directional cosines of the magnetization during measurement and during annealing, respectively. The values for the constants F and G deduced from our measurements are given in Table 1. In the same table the value of $K_u = \frac{4}{10}F + \frac{3}{10}G$ corresponding to the polycrystal is also shown. It is seen that in anisotropy III the F term prevails, particularly when passing to higher temperatures.

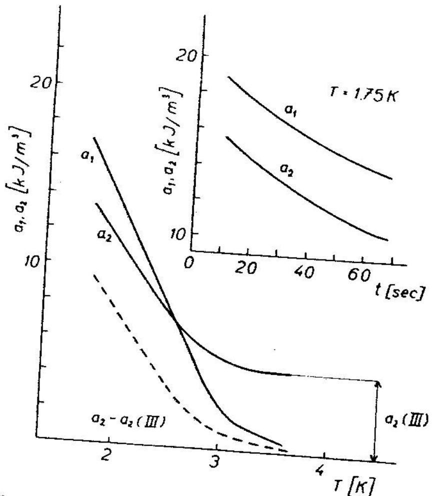

Fig. 9. Temperature and time dependences of Fourier coefficients a_1, a_2 characterizing the unidirectional and uniaxial parts of the torque $L = -a_1 \sin\varphi - a_2 \sin 2\varphi \ldots$ ($Mn_{1.2}Cr_{1.8}O_4$). By a_2 (*III*) the contribution of the process III to a_2 is denoted.

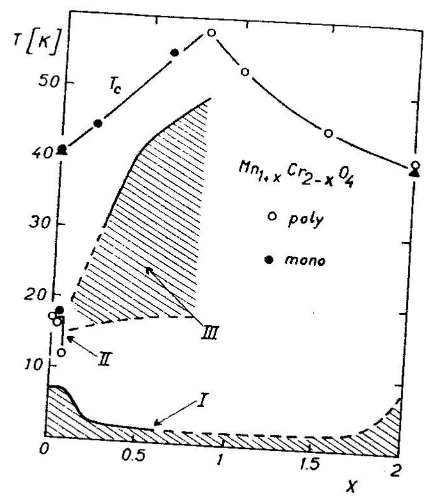

Fig. 10. Critical temperature regions in which anisotropies I, II and III may be induced. For comparison the Curie temperature T_c is also dissplayed.

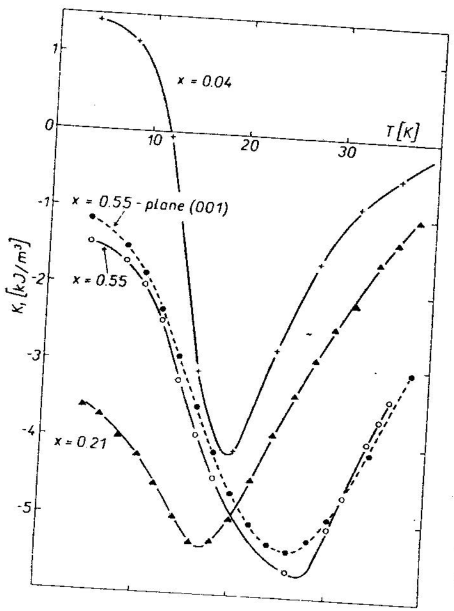

Fig. 11. Temperature dependence of the first magnetocrystalline anisotropy constant K_1 for three cubic samples $Mn_{1+x}Cr_{2-x}O_4$. The full and dashed lines were deduced from the torque measurements in the (110) and (001) planes, resp.

Table 1
Induced anisotropy of type III in the single crystal $Mn_{1.5}Cr_{1.45}O_4$

T [K]	F [kJ/m³]	G [kJ/m³]	G/F	K_u [kJ/m³]
5—15	1.38	1.13	0.82	0.9
25	0.9	0.40	0.44	0.5
38	0.21	0.08	0.38	0.1

IV. DISCUSSION

As already mentioned in § I, the spin configuration of the $Mn_{1+x}Cr_{2-x}O_4$ system is non-collinear in the whole range of x. While the spin arrangement may be taken as known for both end members, the only statement we can make for the cubic compositions with $x > 0$ is that no long range order of transversal spin components does exist and that the local configuration probably represents some compromise between the spiral structure of $MnCr_2O_4$ and the Yafet–Kittel type arrangement in Mn_3O_4. This makes us maintain the following discussion at a rather qualitative or semiquantitative level. It will be primarily oriented towards the induced anisotropy effects and their origin but we shall first briefly discuss the magnetization data.

It is seen from Fig. 4 that in the cubic region the magnetization decreases with an increasing manganese content. This is probably connected with the fact that in the B-sublattice the Cr^{3+} ion (spin $S = 3/2$) *is substituted by the* Mn^{3+} *ion* ($S = 2$). The magnetic moment of the B-sublattice thus increases but the overall magnetization, being directed along the A-sublattice magnetization, decreases. The different behaviour of the magnetic moment in the tetragonal region (Fig. 4) indicates that here the change in the magnetic structure itself dominates over the increase of an average magnetic moment of the B-site ion. This, is, probably, caused by an increase with the x of the mean angle, which the individual B-site magnetic moments make with the magnetization of the B-sublattice. Such an increase may be connected with the increase of the $B-B$ exchange interactions (or, alternatively, with decrease of the $A-B$ interactions) when the spinel structure becomes tetragonally deformed.

From the anisotropy contributions I, II, III, described in paragraph III, I and III are due to the presence of Mn^{3+} and will be discussed first. The Mn^{3+} ion in octahedral environment is known to contribute substantially to the magnetocrystalline anisotropy. This is a consequence of strong orbit-lattice coupling which tends to distort the environment of the ion (the Jahn–Teller effect). The distortions may cooperate (for $x > x_c$) to form a macroscopic tetragonal deformation or may be regarded as quasiindependent ($x < x_c$). In the latter case they could have a dynamic character if the crystal were ideal. In nonhomogeneous systems like solid solutions of the type considered, the distortions are more or less static, due, however, to the stabilization effect of lattice imperfections and accompanying internal stresses. The distortions stabilized in this way may reorient themselves only when the relevant imperfections move. In the presence of magnetization, such a process enables to reach a configuration with minimum energy. When the direction of magnetization is changed, the system of coupled imperfections and the Jahn–Teller distortions will move and reorient itself which leads to a normal type of induced anisotropy. This may be regarded as the source of anisotropy III. Here, the F-term is expected to prevail in (2) as the Jahn–Teller effect leads to an essentially tetragonal distortion for Mn^{3+} in octahedral coordiantion. The origin of the G-term is not clear, it may appear, e.g., as a direct consequence of a simultaneous rearrangement of the lattice imperfections. An estimation of the magnitude of F can be made using the single ion model of anisotropy [33]

$$F = 3DN/\varrho(T)[1 + (kT_A/D)\,\varrho(T_A)], \qquad (3)$$

where D is take axial parameter of the spin hamiltonian of the Mn^{3+} ion, N is the number of ions, T and T_A are temperatures of measurement and annealing, respectively, and $\varrho(T)$ is a function of $y = \exp(g\beta H_{ex}/kT)$,

$$\varrho = (y^4 + y^3 + y^2 + y + 1)/(-y^4 + \frac{1}{2}y^3 + y^2 + \frac{1}{2}y - 1),$$

H_{ex} being the exchange field of the Mn^{3+} spin. Taking. the appropriate value of $D \simeq -3\ \mathrm{cm}^{-1}$, $T_A \simeq 40$ K, $g\beta H_{ex} \simeq 30\ \mathrm{cm}^{-1}$ [34, 35], we obtain $F(T = 10\ \mathrm{K}) \sim 0.43\ \mathrm{cm}^{-1}$/ion. This value is much larger than the experimental one $F = 0.010\ \mathrm{cm}^{-1}$/ion deduced from Table 1, which would mean that only about 2—3 % of Mn^{3+} are active. In the tetragonal region the distortions are stabilized by the cooperative Jahn–Teller effect and their reorientation is prevented. As a consequence, the anisotropy III drops for $x \gtrsim 0.8$ (Fig. 10).

It follows from the above discussion that most of the Jahn–Teller distortions have fixed directions at low temperatures. In this situation another way exists, however, through which the system may lower its energy for a given direction of magnetization and we shall show that its general features are consistent with anisotropy I. Let us notice that in non-collinear spin systems a variety of arrangements usually exists which have the same exchange energy but often differ in anisotropy energy. Hence, if the distribution of the directions of distortions is fixed, the spin system may choose a configuration that minimizes the anizotropy energy without changing the energy of exchange. After turning the magnetization vector another configuration may become stable, spins rearrange and the anisotropy energy relaxes to a new minimum value. As the spin system is directly involved in the relaxation mechanism, the resulting induced anisotropy will generally possess both unidirectional and uniaxial parts. This may be illustrated on

a simple example sketched in Fig. 12. The spin system is supposed to consist of the two sublattices B_1, B_2. The spins within each sublattice are collinear, the sublattice magnetizations making an angle ψ with the overall magnetization M. The anisotropy arises due to the presence of the easy axes ξ_{B_1}, ξ_{B_2}. Let now the crystal rotate around the axis ω, while M is kept fixed by an external magnetic field. For the sake of simplicity we assume that ω is perpendicular to the mirror plane of the

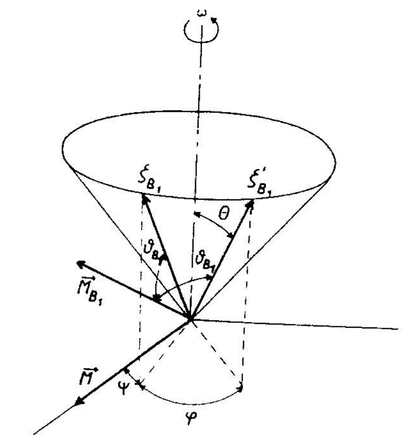

Fig. 12. Model system for the explanation of the origin of the unidirectional anisotropy. For clarity, the quantities related to the B_1 sublattice only are shown.

system considered. If the rotation is much more rapid, compared with the relaxation rate of the spin system, the directions of the sublattice magnetizations remain unchanged. The symmetry of the system implies the form of the anisotropy energy

$$E_a = K_{B_1}\cos^2\vartheta_{B_1} + K_{B_2}\cos^2\vartheta_{B_2}, \qquad (4)$$

where K_{B_1}, K_{B_2} are the anisotropy constants for each sublattice and ϑ_{B_1}, ϑ_{B_2} are the angles which the sublattice magnetization makes with the corresponding easy axis. Due to the symmetry $K_{B_1} = K_{B_2} = K$ and

$$\cos\vartheta_{B_1} = \cos\vartheta_{B_2} = \cos\psi\cos\varphi\sin\Theta + \sin\psi\cos\Theta, \qquad (5)$$

where φ is the angle of rotation and Θ is the angle between ω and the easy axes. Inserting (5) into (4) we obtain

$$E_a = K_0 + K_1\cos\varphi + K_2\cos^2\varphi. \qquad (6)$$

where $K_0 = K\sin^2\psi\cos^2\Theta$, $K_1 = \frac{1}{2}K\sin^2\psi\sin 2\Theta$, $K_2 = K\cos^2\psi\sin^2\Theta$. The anisotropy thus contains both uniaxial and unidirectional terms. Let us note that this model should apply to Mn_3O_4 for explaining its anisotropy in the basal plane provided the spin arrangement described by Jensen and Nielsen [20] is adopted; B_1, B_2 are then identified with the sublattice of what is called in [20] nondoubling spins and ξ_{B_1}, ξ_{B_2} are their local pseudotrigonal axes. To our knowledge no other mechanism was proposed to explain this anisotropy. The crucial point of the applicability of the above model would be the observation of a unidirectional component of the anisotropy.

Coming back to our solid solutions $0<x<2$ we see that anisotropy I

1) possesses unidirectional and uniaxial parts of comparable magnitudes,
2) increases with the content of Mn^{3+},
3) may be almost equally induced in any crystallographic direction,
4) relaxes rapidly even at low temperatures,
5) the relaxation has not a simple diffusion character.

All these features are compatible with the above described model. Point 2) follows from the single ion character of the anisotropy. The maximum value of anisotropy I, which may be obtained for a polycrystalline sample on the basis of our model, was estimated to be 1—3 cm^{-1}/ion (see Appendix A). This is to be compared with the value 0.6 cm^{-1}/ion deduced from Fig. 7. The point 3) may be understood when we realize that there is always a large number of exchange-degenerate configurations. Their number is 32 for Mn_3O_4 and is expected to increase when the long range spin order is destroyed. In the latter case relatively small spin clusters rearrange themselves quasi-independently and the overall relaxation should be fast. When approaching the end members of the system, these clusters become larger and the relaxation is expected to slow down. This is just what we have experimentally observed (Figs. 6, 7). The behaviour mentioned in (5) seems to be connected with the multilevel character of the system and is discussed in Appendix A.

Before concluding the discusssion of anisotropy I we mention another mechanism which might contribute to it and influence the results. Let us suppose that some spin clusters are not turned when the overall magnetization is rotated, due to their strong local anisotropy. Such clusters would be a source of aditional torque of a unidirectional character, There are two main reasons, however, for which we do not believe that anisotropy I may be explained by this mechanism. First, we did not observe any relaxation of magnetization after changing its direction, secondly, the presence of a uniaxial anisotropy term in I could be hardly explained then. On the other hand, in the tetragonal region the lack of technical magnetic saturation may quantitatively modify the results.

The existence of anisotropy II is conditioned by the presence of the long range spiral spin order concerning both the temperature and the composition (Fig. 7, 10). As shown in Appendix B, it may be explained as arising from the single ion contribution of Cr^{3+}, taking into account that the magnetic spiral lowers the symmetry from cubic to orthorhombic.

V. CONCLUSIONS

A thorough investigation of the induced anisotropy effects in the whole system $Mn_{1+x}Cr_{2-x}O_4$, $0\leq x\leq 2$ has shown that three anisotropy contributions may be distinguished; the largest (I) is connected with the rearrangement of the non-collinear spin system, it increases with the Mn^{3+} content and amounts to $\approx 0.6\ cm^{-1}$ per Mn^{3+} ion. It relaxes fast even at low temperatures, giving rise to a large rotational hysteresis. Another contribution (II) is intimately related to the long range-order spiral in stoichiometric (or nearly stoichiometric) $MnCr_2O_4$. The last induced anisotropy contribution (III) was ascribed to reorientations of the local Jahn–Teller distortions around Mn^{3+} ions and it becomes strong in the composition region near the cubic-tetragonal transition only.

To obtain a more detailed picture of the process leading to anisotropy I, an experimental study at temperatures below 2 K would be desirable. Finally, for a quantitative test of the models proposed the detailed knowledge of the spin structure, especially that of the canting angles, would be necessary.

ACKNOWLEDGEMENT

The authors wish to thank Ing. E. Pollert and Ing. M. Nevřiva for the preparation of samples, Dr. P. Novotný for carrying out the measurements in pulse fields, and Dr. A. N. Bazhan (Institute of Physical Problems, Moscow) for making our measurements on the vibrational magnetometer possible.

APPENDIX A
Anisotropy I

We first attempt to estimate roughly the magnitude of I. To this end a simple model will be used, which is based on the following four assumptions:

1) The spin structure is not collinear, the spin of each Mn^{3+} ion making the angle ψ with the direction of the overall magnetization.

2) For each Mn^{3+} ion a local, easy-type axis exists, the anisotropy energy being of the form

$$E_a = k\cos^2\Theta, \tag{A1}$$

where Θ is the angle between the easy axis and the corresponding spin.

3) The number of spin configurations which have the same exchange energy is so large that during the annealing it enables each Mn^{3+} spin to make the smallest possible angle with its easy axis, within the limitation imposed by 1),

4) When the crystal is quickly turned, the magnetization vector as well as the spin configuration remain fixed.

The change of the anisotropy energy, when the crystal is rotated around the axis ω, may be conveniently calculated in the coordinate system with the axis $\omega \| [001]$, $M \| [100]$. If we denote in this system the polar and azimuthal angles of the easy axis by φ_a, ϑ_a, those of the corresponding spin by φ, ϑ and the angle of rotation around ω by Φ, the anisotropy energy (A1) as a function of Φ takes the form

$$E_a = a_1 \cos \Phi + a_2 \cos 2\Phi + b_1 \sin \Phi + b_2 \sin 2\Phi, \tag{A2}$$

where

$$a_1 = \frac{k}{2} \cos(\varphi - \varphi_a) \sin 2\vartheta \sin 2\vartheta_a$$

$$b_1 = \frac{k}{2} \sin(\varphi - \varphi_a) \sin 2\vartheta \sin 2\vartheta_a$$

$$a_2 = \frac{k}{2} \cos 2(\varphi - \varphi_a) \sin^2\vartheta \sin^2\vartheta_a$$

$$b_2 = \frac{k}{2} \sin 2(\varphi - \varphi_a) \sin^2\vartheta \sin^2\vartheta_a. \tag{A3}$$

As expected, the anisotropy energy (A2) has both unidirectional and uniaxial components. Assumptions (1), (3) and (4) of our model provide us with equations from which the angles φ, ϑ may be determined as functions of φ_a, ϑ_a and the canting angle ψ.

$$\cos\varphi \sin\vartheta = \cos\psi \tag{A4}$$

$$\sin\varphi \sin\vartheta \cos\vartheta_a - \cos\vartheta \sin\varphi_a \sin\vartheta_a = 0. \tag{A5}$$

In the polycrystalline samples we have to average (A3) over all the possible directions of the easy axes

$$a_j(pol) = \frac{1}{4\pi} \int_0^{2\pi} d\varphi_a \int_0^{\pi} d\vartheta_a \sin\vartheta_a a_j$$

$$b_j(pol) = \frac{1}{4\pi} \int_0^{2\pi} d\varphi_a \int_0^{\pi} d\vartheta_a \cos\vartheta_a b_j. \quad j = 1,2 \tag{A6}$$

With (A3) — (A6) it may be shown that

$$b_1(pol) = b_2(pol) = 0. \tag{A7}$$

For the estimation of $a_j(pol)$ $(j = 1, 2)$ (A6) was integrated numerically taking

$\psi = 111°$, which is the value of the canting angle in the hausmanite [20]. The result is

$$a_1(pol) = 0.26\,k \qquad a_2(pol) = 0.15\,k. \tag{A8}$$

Within the single ion model of anisotropy at absolute zero temperature

$$k = 3D. \tag{A9}$$

Taking as in paragraph IV (see discussion of process III) $D \approx -3\ \mathrm{cm}^{-1}$, the final estimate is obtained

$$a_1(pol) \approx -2.3\ \mathrm{cm}^{-1}/\mathrm{ion}, \qquad a_2(pol) \approx -1.3\ \mathrm{cm}^{-1}/\mathrm{ion}. \tag{A10}$$

The first and second Fourier coefficients of the torque $L = -\partial E_{an}/\partial\Phi$ have, therefore, about the same magnitude which was also found experimentally. On the other hand, the values (A10) are much higher than those suggested by our experimental results. This may be understood as, due to the assumptions (4) and especially (3), our model gives an upper limit for the magnitude of I.

As already mentioned in paragraph IV, the relaxation behaviour of I does not have a simple diffusion character. We believe that the reason is that when the crystal is turned, more than one state of the spin system will in general possess an energy lower than the energy of the annealed spin configuration. The relaxation then proceeds via many levels having thus a multichannel and cascading character. It is beyond the scope of the present paper to analyse this situation mathematically, instead we will give only a description of the case with the single relaxation time. The experiment which we consider (and which includes most experimental procedures used) may be described as follows: for the time $-\infty < t < 0$ the crystal in annealed in a magnetic field which has a fixed direction, with respect to the crystal. For $0 \leq t \leq t_1$ the crystal is rotated with a constant speed ω, while for $t > t_1$ it is again at rest. For simplicity we treat only the polycrystals in which the induced anisotropy energy has the form

$$E_{an} = c_1 \cos(\Phi - \psi) + c_2 \cos 2(\Phi - \psi), \tag{A11}$$

where ψ, Φ are the angles which the magnetization vector forms with an arbitrary but fixed direction during the annealing and the measurement, respectively. Following closely the procedure used by Broese van Groenou [31], we obtain for the corresponding torque

$$L = 2c_2 \frac{2\omega\tau}{1 + (2\omega\tau)^2} [2\omega\tau e^{-t/\tau} \sin 2\Phi - e^{-t/\tau} \cos 2\Phi + \Omega(t)] +$$

$$+ c_1 \frac{\omega\tau}{1 + (\omega\tau)^2} [\omega\tau e^{-t/\tau} \sin\Phi - e^{-t/\tau} \cos\Phi + \Omega(t)], \tag{A12}$$

where τ is the relaxation time and

$$\Omega(t) = \left\langle \begin{matrix} 1 \\ e^{-(t-t_1)/\tau} \end{matrix} \right. .$$

The unidirectional and uniaxial anisotropy components give, therefore, very similar contribution to the torque. The first two terms in each bracket give rise to an exponentially decaying angular variation of the torque, while the third term, which is constant for $t < t_1$, describes the rotational hysteresis. The quantity ΔL (Fig. 1) is then given by

$$\Delta L = 2\left[2c_2 \frac{2\omega\tau}{1+4\omega^2\tau^2} + c_1 \frac{\omega\tau}{1+\omega^2\tau^2}\right]; \tag{A13}$$

ΔL depends on temperature mainly because of the temperature dependence of the relaxation time. Considering ΔL as a function of $\omega\tau$ we see that at 0 K ΔL is zero ($\omega\tau \to +\infty$), it acquires a maximum for some value of $\omega\tau \in \langle 1/2, 1\rangle$ (position of the maximum depending on the ratio c_1/c_2) and decreases to zero when the temperature is increased ($\omega\tau \to 0$). This is the behaviour experimentally observed (Fig. 6). However, with a single relaxation time we were unable to explain simulteneously the $\Delta L(\omega)$ and $\Delta L(T)$ dependences. A thorough analysis shows that this difficulty may be overcome if, instead of a single τ, the distribution of relaxation times is considered.

Another difficulty, which leads us to believe that the description of I by the diffusion process is insufficient, is that the decay of the angular dependence of the torque ($0 < t < t_1$) is much more rapid than the decay of the torque after stopping the rotation ($t > t_1$). From (A12) if follows that the diffusion theory predicts the same rate of decay and this cannot be altered whatever distribution of the relaxation times is assumed. We conclude, therefore, that for a full description of the relaxation of I a more sophisticated analysis is desirable.

APPENDIX B

Anisotropy II

In $MnCr_2O_4$ each Cr^{3+} ions is situated in a trigonally distorted octahedron. There are four crystallographically equivalent octahedral sites B_k ($k = 1, 2, 3, 4$), which differ in the direction of the trigonal axis (Fig. 13). If we use the molecular field approximation for the echange, the spin-hamiltonian of Cr^{3+} at the kth site may be written in the form

$$\varkappa_k = g\beta H_{ex}^{(k)} S^{(k)} + D\left[S_{\xi_k}^2 - \frac{1}{3}S(S+1)\right], \tag{B1}$$

where $H_{ex}^{(k)}$ is the exchange field, ξ_k is the trigonal axis of the k-th ion. The contribution to the anisotropic part of the free energy, which corresponds to (B1) as determined in a usual way [33], is

$$f_k = R(T)\cos^2\vartheta_k, \tag{B2}$$

where ϑ_k is the angle, which the trigonal axis ξ_k forms with the exchange field $H_{ex}^{(k)}$, $R(T)$ is the function of $y = e^{g\beta H_{ex}/kT}$

$$R(T) = 3D\frac{y^3 - y^2 - y + 1}{y^3 + y^2 + y + 1}. \tag{B3}$$

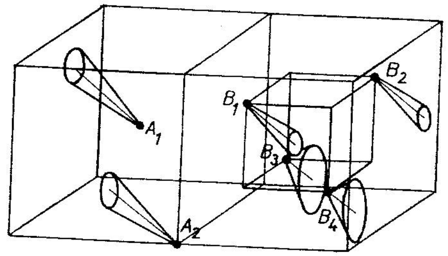

Fig. 13. Cation sites in the primitive cell of $MnCr_2O_4$. The magnetic moments from conical spirals with a common propagation vector lying in the direction close to the cone axes $\langle 110\rangle$.

To obtain the overall anisotropy energy, (B2) must be summed over all the Cr^{3+} ions. In a cubic spinel such a summation would give simply a constant as $\sum_{k=1}^{4}\cos^2\vartheta_k = 4/3$. In our case, however, the spin arrangement lowers the cubic symmetry to an orthorhombic one. As shown in Fig. 13, the cones on which the Cr^{3+} spins lie have two different values of the top angle. The orthorhombic axes go through the sites having the same top angle. There are six different ways in which the orthorhombic axis may be chosen, to each set of the axis there corresponds amagnetically different phase of $MnCr_2O_4$. The summation of (B2) then gives the result

$$\begin{aligned} F_{12} &= c\alpha_x\alpha_y \qquad & F_{23} &= -c\alpha_x\alpha_y \\ F_{13} &= c\alpha_x\alpha_y \qquad & F_{23} &= -c\alpha_x\alpha_y \\ F_{14} &= c\alpha_x\alpha_z \qquad & F_{34} &= -c\alpha_y\alpha_z \end{aligned} \tag{B4}$$

F_{jk} is the anisotropic part of the free energy of the phase in which the sites B_j and B_k have the same cone angle β_1, α_x, α_y, α_z are the direction cosines of magnetization. The constant c is

$$c = \frac{RN}{2}(\cos^2\beta_1 - \cos^2\beta_2), \tag{B5}$$

where R is given by (B3), N is the number of Cr^{3+} ions. If the six phases occur with the same probability, no anisotropy appears. However, the annealing of the system in an external magnetic field stabilizes the phase with the lowest anisotropy energy and the annealed system possesses the orthorhombic anisotropy.

In polycrystalline samples an averaging procedure of the free energy is to be performed. We have assumed that in each crystallite only a single phase with the lowest energy is formed. The calculation then leads to the result

$$F = c\,\frac{3\sqrt{3}}{4\pi}\cos 2\Phi, \qquad \text{(B6)}$$

where Φ is the angle which the magnetization direction forms during annealing with the one at the moment of measurement.

In spinels the EPR of the Cr^{3+} ion gives the value of $D \sim (0.5-1)\ \mathrm{cm}^{-1}$. The main uncertainty then arises from the values of the cone angles. While the NMR [16] gives $\beta_1 = 94°$, $\beta_2 = 97°$ and $\cos^2\beta_1 - \cos^2\beta_2 = 0.01$, the neutron diffraction leads to considerably different values $\beta_1 = 27°$, $\beta_2 = 77°$ [12] and $\cos^2\beta_1 - \cos^2\beta_2 = 0.74$. We can thus only conclude that the value of the parameter c is of the order of 0.2—100 $\mathrm{kJ/m^3}$. The magnitude of the observed anisotropy lies within the scope of these values.

REFERENCES

[1] Irani, K. S., Sinha, A. P. B., Biswah, A. B.: J. Phys. Chem. Sols. *23* (1962), 711.
[2] Brabers, V. A. M.: *Thesis.* Technical University Eidhoven 1970.
[3] Shet, S.G.: *Thesis.* University of Poona 1970.
[4] Holba, P., Khilla, M. A., Krupička, S.: J. Phys. Chem. Sols. *34* (1973), 387.
[5] Holba, P., Neřiva, M. Pollert, E.: Mat. Res. Bull. *10* (1975), 853.
[6] Pollert, E. Holba, P., Nevřiva, M., Novák, K.: J. Phys. Chem. Sols. *38* (1977), 1145.
[7] See, e.g., Goodenough: *Magnetization and the Chemical Bond.* Interscience Publishers, J. Willey and Sons, New York—London 1963.
[8] Pollert, E., Jirák, Z.: Czech. J. Phys. B *26* (1976), 481.
[9] Miller, A.: J. appl. Phys. *30* Suppl. (1959), 24S.
[10] Blasse, G.: Philips Res. Repts. Supplements. 1964, No. 3.
[11] Jirák, Z., Vratislav, S., Zajíček, J.: Phys. Stat. Sol. (a) *37* (1976), K47.
[12] Hastings, J. M., Corliss, L. M.: Phys. Rev. *126* (1962), 556.
[13] Dwight, K., Menyuk, M., Feinleib, J., Wold, A.: J. appl. Phys. *37* (1966), 962.
[14] Plumier, R.: Comptes Rendus B *265* (1967), 726.
[15] Vratislav, S., Zajíček, J., Jirák, Z., Andersen, A. F.: J. Magn. and Magn. Mat. *5* (1977), 41.
[16] Nagasawa, H., Tsushima, T.: Phys. Letts. *15* (1965), 205.
[17] Lyons, D. J., Kaplan, T.A., Dwight, K., Menyuk, N.: Phys. Rev. *126* (1962), 540.
[18] Hasper, J. S.: Bull. Am. phys. Soc. *4* (1959), 888.
[19] Boucher, B., Buhl, R., Perrin, .: J. Phys. Chem. Sols. *32* (1971), 2529.

[20] Jensen, G. B., Nielsen, O. V.: J. Phys. C *7* (1974), 409.
[21] Jirák, Z., Vratislav, S. Zajíček, J.: Phys. Stat. Sol. (a) *50* (1978), K 131.
[22] Miyahara, S., Miyadai, T.., Horiuti, S.: J. Phys. (Paris) *32* (1971), C 1.
[23] Krupička, S., Roskovec, V., Zounová, F., Nevřiva. M.: *Proc. ICM '73.* Publ. House Nauka, Moscow 1974, p. 223.
[24] Krupička, S., Roskovec, V., Zounová, F.: 4th *Conf. of Czechosl. Physicists.* Academia, Prague 1976, p. 593.
[25] Krupička, S., Jirák, Z., Novák, P., Roskovec, V., Zounová, R.: Physica *86—88 B* (1977), 1459.
[26] Nevřiva, M.: Kristall und Technik *6* (1971), 517.
[27] Novák, J., Pollert, E.: Z. anal. Chem. *283* (1977), 363.
[28] Gerber, R., Vilím, F.: J. Sci. Instr. J. Phys. E *1* (1968), 389.
[29] Bělov, K. P.: *Magnitnyje prevraščenija.* GIFML Moscow 1959.
[30] Dietzmann, G.: *Wiss. Zeits. Karl.-Marx-UNiversität.* Leipzig (1965), 821; Dietzmann, G., Michalk, C.: Phys. Stat. Sol. *8* (1965), K 258.
[31] Broese van Groenou, A., Pearson, R. F.: J. Phys. Chem. Sols. *28* (1967), 1017.
[32] See, e.g., Jacobs, I. S., Luborskx, F. E.: J. appl. Phys. *28* (1957), 467.
[33] Novák, P.: Czech. J. Phys. B *16* (1966), 723.
[34] Gerber, R., Elbinger, G.: J. Phys. C *3* (1970), 1363.
[35] Nielsen, O. V.: J. Phys. C *9* (1976), 1307.

Received January 7th, 1980.